Topology in $U(N_c)$ Lattice Gauge Theories in 2D

Philip Rouenhoff and Stephan Dürr

BERGISCHE UNIVERSITÄT WUPPERTAL

Motivation

In two dimensions, $U(N_c)$ gauge theory has non-trivial topology due to the $U(1)$-factor in $U(N_c) = U(1) \rtimes SU(N_c)$. This leads to the algorithmic problem of topological freezing just like in 4D $SU(3)$, see Fig. 1.

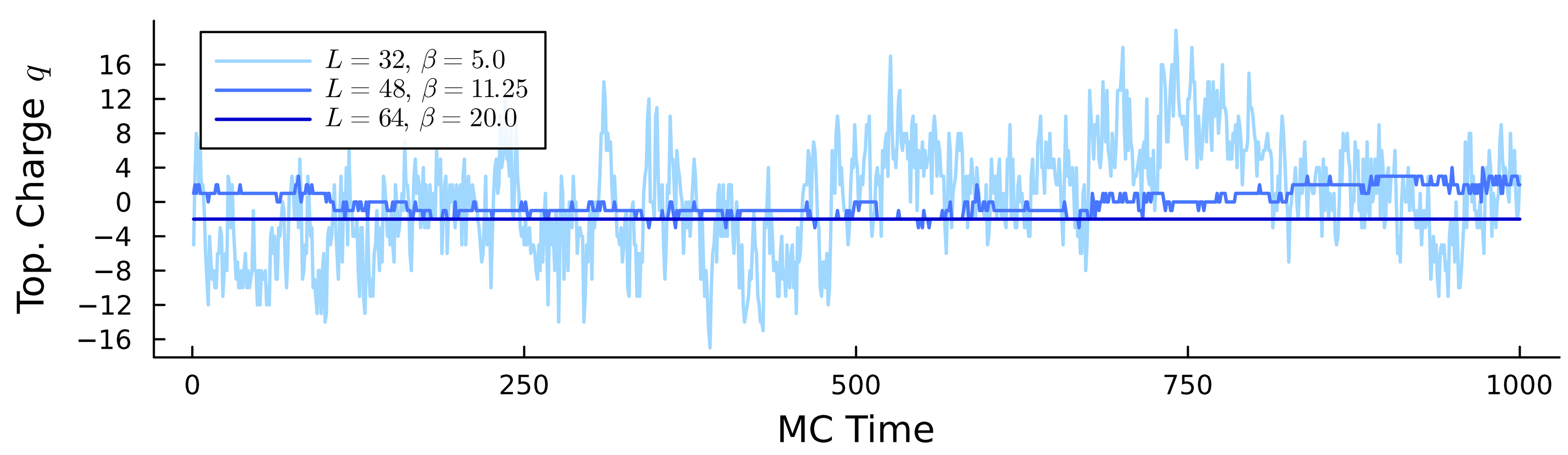

Figure 1. Time series of the topological charge q in 2D $U(2)$ on different lattices of the same line of constant physics: the finer, the stronger the topological freezing.

A convenient, integer-valued definition for the topological charge q is given in Eq. (1). For $U(2)$ in 2D one can show that the topological susceptibility χ_{top} takes the form of Eq. (3), which agrees with numerical results in Fig. 2. $SU(N_c)$ theory is topologically trivial in 2D.

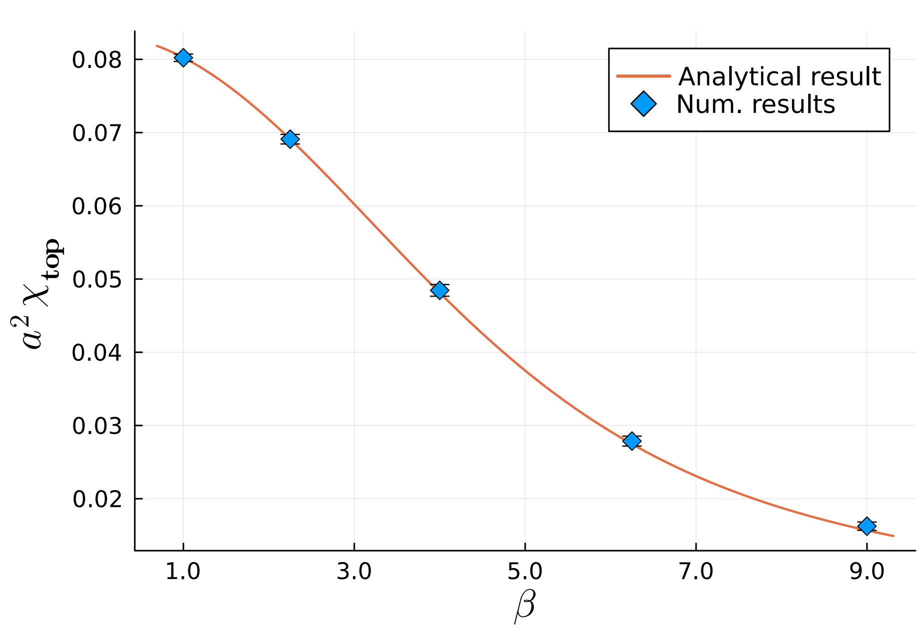

Figure 2. Comparison of analytical and measured topological susceptibility for $U(2)$.

$$q \equiv \frac{1}{2\pi}\sum_{n\in\Lambda} \mathfrak{Im}\left[\log\det P_{xt}(n)\right] \quad (1)$$

$$\chi_{\text{top}} = \frac{\langle q^2\rangle}{V} \quad (2)$$

$$\chi_{\text{top}}^{U(2)} = \frac{\int_{-\frac{\pi}{2}}^{\frac{\pi}{2}} \mathrm{d}\alpha\ \alpha^2\, \frac{I_1(\beta\cos(\alpha))}{\cos(\alpha)}}{\pi^2 \int_0^{\pi} \mathrm{d}\alpha\ \frac{I_1(\beta\cos(\alpha))}{\cos(\alpha)}} \quad (3)$$

$$\chi_{\text{top}}^{SU(N_c)} = 0 \quad (4)$$

Global Minima per Sector: $N_c = 2$

Instanton-like solutions in 2D QED on the lattice are given in *[J. Smit, J. Vink, Nucl. Phys. B, vol. 286, 1987]* as

$$U_x(x,t) = e^{-it\frac{2\pi q}{N_x N_t}}, \quad U_t(x,t) = e^{ix\frac{2\pi q}{N_x}\delta_{t,N_t}}. \quad (5)$$

In the case of $U(2)$ one can embed the $U(1)$-instanton in the following fashion (see Fig. 3):

$$U_x(x,t) = e^{-it\frac{\pi q}{N_x N_t}}\exp(i\vec{u}\vec{\sigma}\,\delta_{x,N_x}), \quad U_t(x,t) = e^{ix\frac{\pi q}{N_x}\delta_{t,N_t}}\exp(i\vec{v}\vec{\sigma}\,\delta_{t,N_t}), \quad (6)$$

where $\vec{u}, \vec{v} \in \mathbb{R}^3$ depend on q:

- for even q: $\vec{u} \parallel \vec{v}$.
- for odd q: $\vec{u} \perp \vec{v}$ and $|\vec{u}| = |\vec{v}| = \frac{\pi}{2}$

Further information on these configurations:

- $P_{xt}(\vec{n}) = e^{i\frac{q\pi}{N_x N_t}}\mathbf{1}\,\forall \vec{n}\in\Lambda$ $\Rightarrow$ minima of the gauge action
- *global* minima of the action: see Fig. 4(b)
- action given by Eq. (7) and plotted in Fig. 4(a)

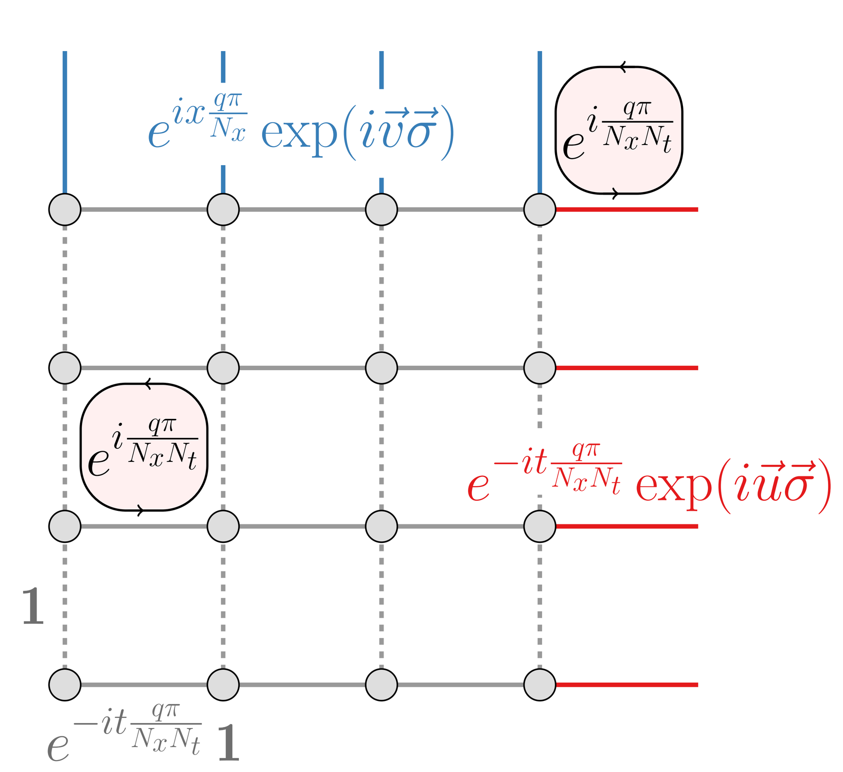

Figure 3. A visualitzation of Eq. (6), the instanton-like solutions for $U(2)$.

$$S^{\mathrm{G}}[U] = \frac{\beta}{2}\sum_{\vec{n}\in\Lambda}\mathfrak{Re}\mathrm{Tr}(\mathbf{1} - P_{xt}(\vec{n})) = \beta N_x N_t\left(1 - \cos\left\{\frac{q\pi}{N_x N_t}\right\}\right). \quad (7)$$

The $U(2)$-instantons are unique up to the following transformations:

- gauge transformations may rotate $\vec{u}$ and $\vec{v}$ (via quatern. representation)
- multiplying the last x- or t-slice (red or blue links in Fig. 3) with an appropriate $g \in U(N_c)$ may stretch $\vec{u}$ and $\vec{v}$ or shift the $U(1)$-phase

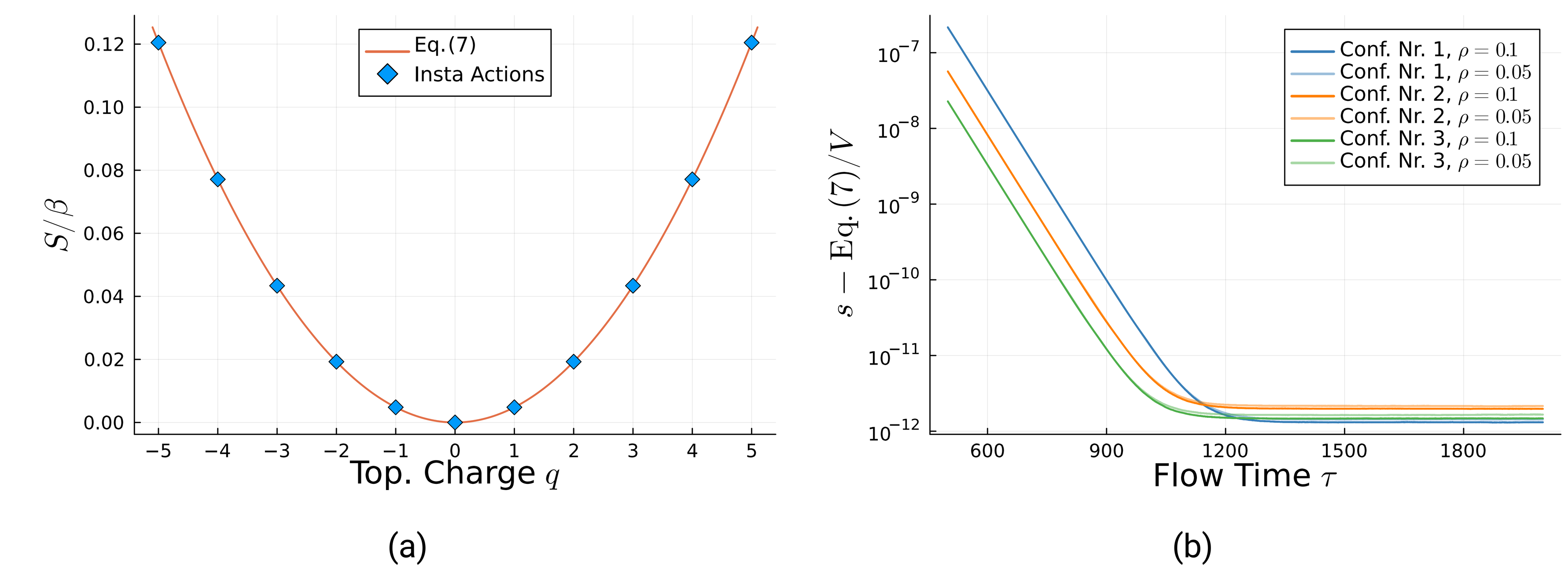

Figure 4. (a) shows the lower bound of the action per topological sector for $N_c = 2$, given by Eq. (7). In (b) configurations of $|q| = 1$ generated during a simulation with $\beta = 6.0$ are stout smeared, and the difference of their action densities to Eq. (7) is plotted against the gradient flow time $\tau = \rho \cdot N_{\text{smear}}$. One can see that up to numeric precision they all converge towards the respective lower bound given of Eq. (7). The lattice sizes used were $N_x = N_t = 32$ in both cases.

Local Minima per Sector

If we only require $\mathfrak{Re}\mathrm{Tr}P_{xt}$ to be the same at every lattice site, as opposed to P_{xt}, we can derive further local minima of the gauge action. In this case it is more straightforward to generalize to $N_c \geq 2$: we adapt the $U(1)$-factor and use the exponential of $\lambda_{N_c^2-1}$, the last generator of $\mathfrak{su}(N_c)$. By minimizing the gauge action of this ansatz, we obtain a solution for each $z \in \mathbb{Z}$:

$$U_x(x,t) = e^{-it\frac{2\pi q}{N_c}\frac{1}{N_x N_t}}\exp\left(-it\frac{2\pi}{N_t N_x}\sqrt{\frac{N_c^2 - N_c}{2}}\left(z - \frac{q}{N_c}\right)\lambda_{N_c^2-1}\right) \quad (8a)$$

$$U_t(x,t) = e^{ix\frac{2\pi q}{N_c}\frac{1}{N_x}\delta_{t,N_t}}\exp\left(ix\frac{2\pi}{N_x}\sqrt{\frac{N_c^2 - N_c}{2}}\left(z - \frac{q}{N_c}\right)\delta_{t,N_t}\lambda_{N_c^2-1}\right). \quad (8b)$$

Fig. 5(a) shows the actions of these local minima, given by:

$$\mathfrak{Re}\mathrm{Tr}P_{xt} = (N_c - 1)\cos\left(\frac{2\pi z}{N_x N_t}\right) + \cos\left(\frac{2\pi}{N_x N_t}\Big(q - (N_c - 1)z\Big)\right). \quad (9)$$

While Fig. 5(b) suggests that these configurations may actually be saddle points, Fig. 5(c) shows that they are metastable with respect to cooling.

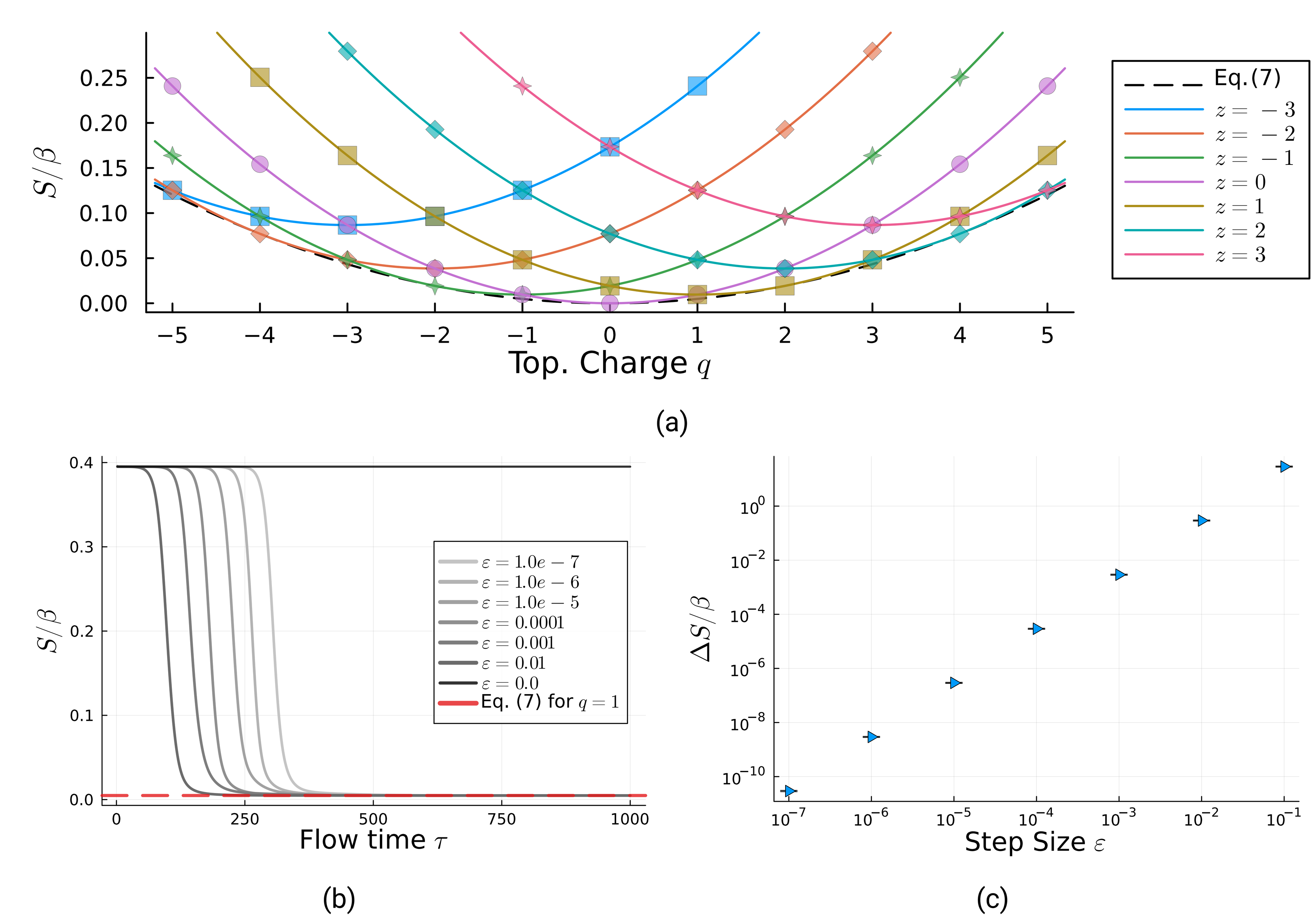

Figure 5. In (a) the actions of the local minima in Eq. (8) are plotted for various values of z for $U(2)$. In (b) each link of the $(z = 5)$-configuration at $q = 1$ was multiplied with a random $U(2)$-element of Metropolis-step size ϵ and then flowed. The smaller ϵ, the longer it takes to flow into the sector minimum given by Eqs. (6) and (7). The $(\epsilon = 0.0)$-curve shows that the local minima are stable stable under gradient flow. In (c) for every ϵ, 1000 Metropolis proposals were generated for the same $(z = 5)$-configuration. The action difference ΔS is strictly positive for any ϵ. The lattice sizes used were $N_x = N_t = 32$ in all cases.

Note that for $q = N_c$ resp. $q = 2$ both Eqs. (6) and (8) yield configurations whose links are proportional to $\mathbf{1}$ (or equivalent to such configurations), the most straightforward embedding of the $U(1)$-instanton (5).

philip.rouenhoff [at] uni-wuppertal.de